Journal of Materials Chemistry C

ROYAL SOCIETY OF CHEMISTRY

COMMUNICATION

View Article Online
View Journal | View Issue

Cite this: J. Mater. Chem. C, 2024, 12, 15413

Received 26th July 2024,
Accepted 15th September 2024

DOI: 10.1039/d4tc03204g

rsc.li/materials-c

Lifetime thermometry with an ytterbium(III)–terbium(III) molecular upconverter†

Diogo Alves Gálico and Muralee Murugesu *

In this work, we report the first example of lifetime thermometry with a molecular upconverter. To reach our goal, we synthesized a {$Tb_{10}Yb_{10}$} molecular cluster-aggregate that emits *via* a cooperative upconversion mechanism. The operational temperature of the lifetime-based thermometer is in the 23–45 °C range with a maximum relative sensitivity of 2.26% °C^{-1} at 45 °C.

Upconversion (UC) is a fascinating phenomenon in which the pilling up of two or more low-energy photons results in the emission of higher-energy photons.[1–3] Unlike the nonlinear optics processes such as second-harmonic generation, UC is based on multiple first-order absorption processes such as excited-state absorption (ESA), energy transfer upconversion (ETU), and cooperative upconversion (CUC), showing a higher efficiency than nonlinear processes.

Until the early 2000s, studies of UC emitters were mainly focused on lanthanide (Ln^{III})-based nanoparticles and low-phonon solid materials. Since then, researchers have started investigating the UC process in low-nuclearity Ln^{III}-based molecular complexes.[4–11] The ability of realizing photon UC with molecular systems is expected to overcome some intrinsic issues inherent to nanoparticles. The use of complexes allows exact structure determination due to the molecular nature, enabling structure–property relationship studies, a powerful tool to finely modulate the optical properties. Despite the success of the earlier works in observing UC in molecular species, the use of low-nuclearity compounds resulted in low UC quantum yields (UCQY),[4–11] much below the values observed for nanoparticles and low-phonon solid materials.[12–14]

Recent studies have shown that the use of spherical molecular cluster-aggregates (MCAs) alleviates issues related to the molecular flexibility due to the metal-core rigidity of MCAs, reducing non-radiative vibrational quenching.[15–18] Additionally, the presence of a large number of Ln^{III} atoms within the molecular structure of MCAs allows for a meticulous control of the energy-transfer (ET) processes *via* composition control. Hence, these systems are ideal candidates for the realization of high-performance molecular UC.[19–24]

Even though several reports have demonstrated molecular UC with different systems, the consolidation of molecular upconverters is still in the early stages, with studies mostly dealing with the demonstration of UC in complexes and MCAs.[4–11] Therefore, we truly believe that an important step to establish molecular upconverters as a viable alternative to nanoparticles and low-phonon materials is to migrate from purely demonstrating UC emission to rationalizing and demonstrating a proof-of-concept for potential applications.

The first demonstration of ratiometric luminescence thermometry with molecular upconverters was conducted by our group.[20] By synthesizing the {$Gd_{11}Tb_2Yb_7$} MCA and subsequently replacing the Gd^{III} atoms with Eu^{III}, we obtained the {$Eu_8Gd_3Tb_2Yb_7$}, {$Eu_9Gd_2Tb_2Yb_7$}, {$Eu_{10}Gd_1Tb_2Yb_7$}, and {$Eu_{11}Tb_2Yb_7$} MCAs, all displaying strong temperature dependent Tb^{III} → Eu^{III} ET, excited *via* the CUC mechanism, and showcasing excellent luminescent thermometry capabilities.

Herein, we present the first demonstration of lifetime thermometry using a molecular upconverter. This approach has the advantage of mitigating issues related to intensity variations and power fluctuations of the excitation source, common in other luminescence thermometry methods.[25–27] To achieve our objectives, we synthesized the {$Tb_{10}Yb_{10}$} MCA (Fig. 1a and Fig. S1, ESI†). Our choice of composition is inspired by the work of the Charbonnière group,[23] which showed that having a similar number of donor (Yb^{III}) and acceptor (Tb^{III}) atoms in molecular CUCs enhances the UCQY. This is contrary to ETA UC with Yb^{III}/Er^{III} and Yb^{III}/Ho^{III} pairs, where an excess of donors is optimal.[12–14]

The heterometallic {$Tb_{10}Yb_{10}$} MCA was prepared following our previously reported procedure (ESI†).[17–20] Powder X-ray diffractograms (PXRD) confirm that the compounds are isostructural to the icosanuclear {Ln_{20}} MCA, which crystallizes in

Department of Chemistry and Biomolecular Sciences, University of Ottawa, 10 Marie Curie, Ottawa, Ontario, K1N 6N5, Canada.
E-mail: m.murugesu@uottawa.ca

† Electronic supplementary information (ESI) available: Experimental procedures and additional characterization. See DOI: https://doi.org/10.1039/d4tc03204g

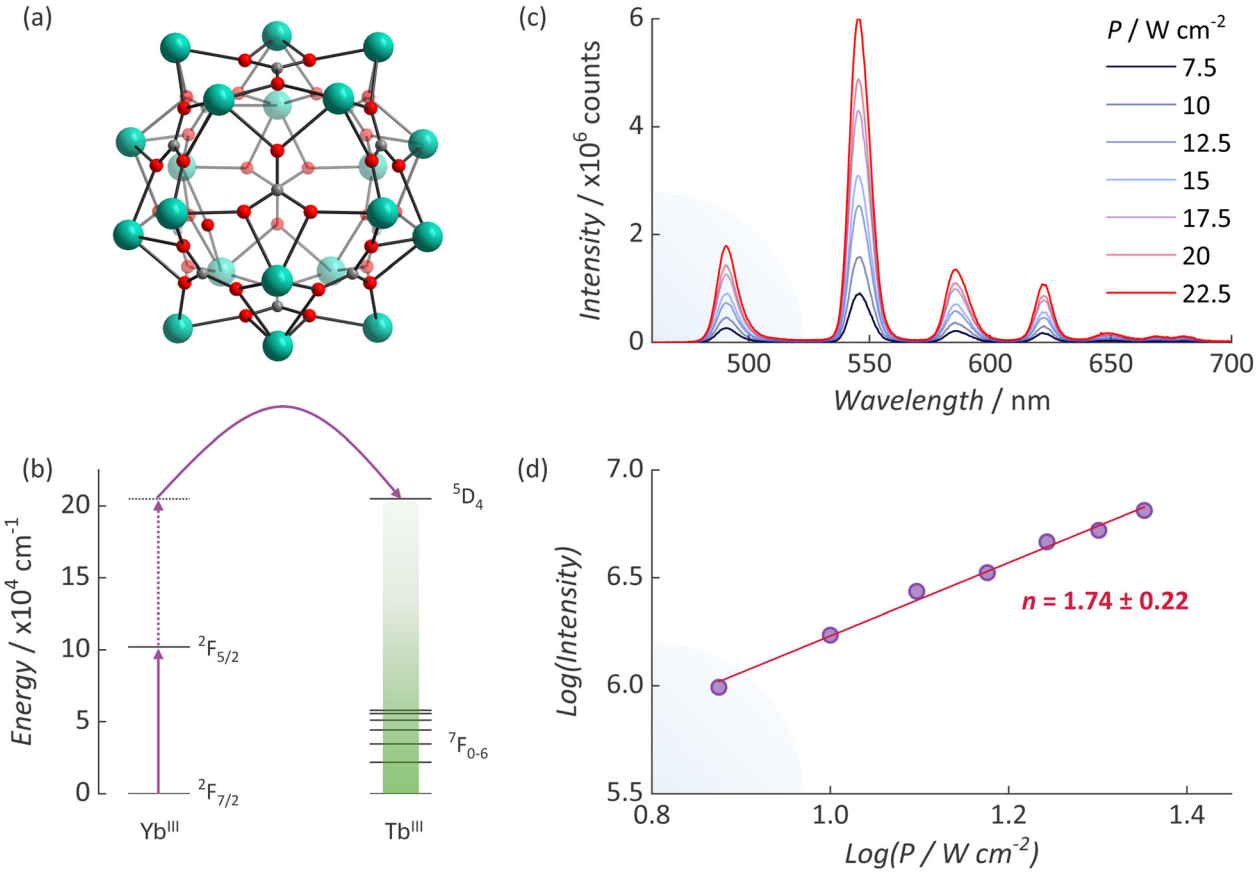

Fig. 1 (a) Molecular core structure of **{Ln$_{20}$}** MCA. Color code: cyan for Ln^{III}, grey for carbon, and red for oxygen. (b) Partial energy level diagram for the MCA depicting Yb^{III} and Tb^{III} levels and the CUC mechanism. (c) Power dependent upconversion spectra for a 0.1 mg mL^{-1} deuterated methanol solution of **{Tb$_{10}$Yb$_{10}$}** obtained at 25 °C (λ_{exc} = 980 nm/ν_{ex} = 10 204 cm^{-1}); see Fig. S4 (ESI†) for the transition labels. (d) Log–log plots of the emission intensities as a function of the incident pump power for **{Tb$_{10}$Yb$_{10}$}** indicating two photon upconversion (n = 1.74).

the $R\bar{3}$ (# 148) space group (Fig. 1a and Fig. S1, S2, ESI†). The Fourier transform infrared (FTIR) spectrum shows the expected molecular vibrations (Fig. S3, ESI†). ICP-OES supports the nominal chemical composition, with a good agreement between the theoretical and experimental Ln^{III} ratio. Further experimental details are available in the ESI.† Photoluminescent studies were carried out in deuterated methanol (0.1 mg mL^{-1}), as the solubility and the stability of the **{Ln$_{20}$}** MCAs in this solvent has previously been demonstrated by NMR spectroscopy.[19,20]

Excitation of **{Tb$_{10}$Yb$_{10}$}** at 980 nm (7.5–22.5 W cm^{-2} power density range), resonant with the Yb^{III} $^2F_{5/2}$ excited state results in the characteristic green emission from the Tb^{III} ion due to the $^5D_4 \rightarrow {}^7F_{6\text{-}0}$ transition bands (Fig. 2b and c and Fig. S4, ESI†). The low power densities employed here exclude the possibility of competitive nonlinear optical processes, and the slope obtained *via* log–log plots[28] (n = 1.74; Fig. 2d) is in good agreement with the presence of two photon UC *via* the CUC mechanism. Absolute UCQY was measured in an integrated sphere as previously reported.[19,20] For **{Tb$_{10}$Yb$_{10}$}**, a UCQY of 4.3 × 10^{-2}% was obtained with an excitation power density of 7.5 W cm^{-2}. This value is two orders of magnitude higher than the value previously observed for the **{Gd$_{11}$Tb$_2$Yb$_7$}** MCA (4.3 × 10^{-2}%),[20] confirming that for the Yb^{III}/Tb^{III} CUC, an equal number of donors and acceptors enhance the UC performance.

Emission decay curves of the Tb^{III} $^5D_4$ emitting state were collected at 25 °C (Fig. 2 and Fig. S5, ESI†) under different excitation pulse widths and show a multiexponential decay profile due to the presence of four different crystallographic sites occupied by Ln^{III} ions within the **{Ln$_{20}$}** asymmetric unit.[17–20] Average lifetime ($\langle\tau\rangle$) values were calculated from the decay curves as expressed by eqn (1),[29,30] where t_0 is the time at which the curve hits its maximum intensity (I) and t_1 is when it reaches the background.

$$\langle\tau\rangle = \frac{\int_{t_0}^{t_1} t \cdot I(t) \cdot \mathrm{d}t}{\int_{t_0}^{t_1} I(t) \cdot \mathrm{d}t} \quad (1)$$

It is noted that the $\langle\tau\rangle$ is highly dependent on the excitation width and consequently, the saturation of the Tb^{III} $^5D_4$ emitter state, ranging from 1.09 ms with a 0.5 ms pulse width to 1.19 ms when a 10.0 ms pulse width is employed and the excited state is completely saturated. In the latter condition, a rising time of 0.34 ms is observed for **{Tb$_{10}$Yb$_{10}$}**. Therefore, we

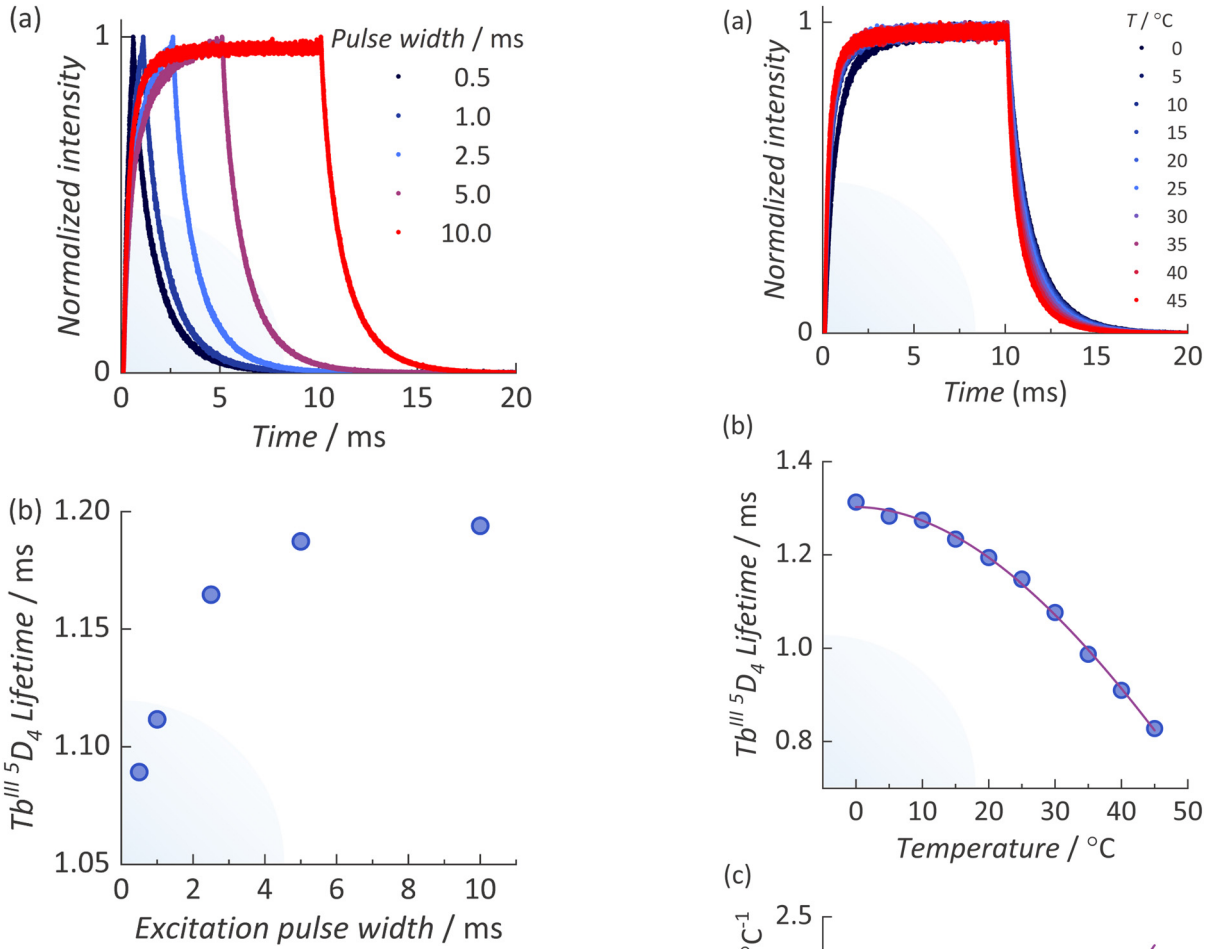

Fig. 2 (a) Emission decay curves obtained at 25 °C monitoring the Tb^{III} $^5D_4$ emitter state (545 nm). (b) Variable excitation pulse width lifetime values obtained at 25 °C.

selected the maximum pulse width (10.0 ms) to perform the lifetime thermometry studies.

Temperature-dependent emission decay curves are shown in Fig. 3a in the 0–45 °C range. It is evident from the emission decay curves that a strong reduction in the $\langle\tau\rangle$ occurs upon increasing the temperature. At 0 °C, an $\langle\tau\rangle$ of 1.31 ms is obtained, while at 45 °C, the value is reduced to 0.83 ms. Hence, we selected the Tb^{III} $^5D_4$ emitter state $\langle\tau\rangle$ as our thermometric parameter (Δ).

The temperature dependence of Δ is shown in Fig. 3b. A logistic function (eqn (2)) was used for the mathematical fitting of the Δ values. It is important to point out that this function has no physical meaning and was used just for fitting purposes. To evaluate the thermometric performance, relative thermal sensitivity (S_R) was obtained by applying the fitted function to eqn (3) (Fig. 3c).[31,32]

$$y = \frac{A_2 + (A_1 - A_2)}{1 + (x/x_0)^p} \quad (2)$$

$$S_R = \frac{1}{\Delta}\left|\frac{\partial \Delta}{\partial T}\right| \quad (3)$$

Fig. 3 (a) Temperature dependence of the emission decay curves obtained at 25 °C monitoring the Tb^{III} $^5D_4$ emitter state (545 nm). (b) Temperature dependence of the Tb^{III} $^5D_4$ average lifetime. (c) Temperature dependence of the relative thermal sensitivities (S_R) for **{$Tb_{10}Yb_{10}$}** MCA.

As can be noted in Fig. 3c, a maximum S_R of 2.26% °C^{-1} is obtained at 45 °C for **{$Tb_{10}Yb_{10}$}** MCA with an operational range, *i.e.*, temperatures in which S_R lies above 1% °C^{-1}, ranging from 23 to 45 °C^{-1}. The operational range for the lifetime-based thermometry with the **{$Tb_{10}Yb_{10}$}** MCA occurs in a biologically important temperature range, indicating the potential that MCAs hold for nanothermometry in biological systems. The present work is the first example of lifetime-based

thermometry with molecular upconverters and the first example of this thermometric approach in a Yb^{III}/Tb^{III} system excited *via* a CUC mechanism.

For a more quantitative analysis of the temperature dependence of the Tb^{III} $^5D_4$ emitter state lifetime we applied a Mott–Seitz model.[33–35] By applying the model involving a single deactivation channel (eqn (4)) a ΔE of 4651 ± 409 cm^{-1} was obtained. As the triplet state of the chp^- ligand is located approximately at 25 000 cm^{-1}, the obtained value is consistent with a deactivation *via* back energy-transfer from the Tb^{III} $^5D_4$ emitter level to the ligand triplet state. The presence of ligand states acting as thermally activated quencher states for the Ln^{III} ion emissions highlights a potential advantage of molecular upconverters when compared to nanoparticles as luminescence thermometers.

$$\tau(T) = \frac{\tau_0}{1 + A\exp(-\Delta E/k_b T)} \quad (4)$$

Another intriguing aspect of the temperature dependent emission decay curves is a clear decrease of the rise time at higher temperatures, indicating a faster ET process (Fig. S6 and S7, ESI†). At 0 °C, a rise time of 0.61 ms is observed, while at 45 °C the rise time is reduced to 0.29 ms. The faster ET process at higher temperatures corroborates Güdel's suggestions that the Yb^{III}/Tb^{III} CUC mechanism is a phonon-assisted process.[36]

Conclusions

In summary, herein we are reporting the first example of lifetime thermometry with a molecular upconverter. This study demonstrates that the MCA upconversion properties can be explored to integrate into optical thermometric approaches, namely the lifetime thermometry. With a **{$Tb_{10}Yb_{10}$}** MCA, we are able to obtain UC after exciting the Yb^{III} $^2F_{5/2}$ excited state with a 980 nm laser, resulting in the characteristic Tb^{III} green emission. The UC occurs *via* the CUC mechanism and **{$Tb_{10}Yb_{10}$}** shows an UCQY of 4.3 × 10^{-2}%.

Temperature-dependent emission decay measurements reveal a strong temperature dependence of the Tb^{III} $^5D_4$ emitter level lifetime, enabling us to realize lifetime-based thermometry with a molecular upconverter. A maximum relative sensitivity of 2.25% $°C^{-1}$ at 45 °C was obtained for **{$Tb_{10}Yb_{10}$}** with an operational range between 23–45 °C, highlighting the potential that molecular upconverters hold for thermometry in the biologically important temperature range. The strong temperature dependence is mediated by a back energy-transfer from the Tb^{III} $^5D_4$ emitter level to the ligand triplet state.

We expect that this work will contribute to moving the attention of the molecular UC community from simply demonstrating new molecular upconverters to rationally targeting potential applications, an important step to consolidate the field of molecular UC.

Data availability

The data that support the findings of this study are available from the corresponding author upon reasonable request.

Conflicts of interest

There are no conflicts to declare.

Acknowledgements

This work was supported by the Canadian Foundation for Innovation and the Natural Sciences and Engineering Research Council of Canada.

Notes and references

1 F. Auzel, *C. R. Acad. Sci.*, 1966, **263**, 819.
2 F. Wang and X. Liu, *Chem. Soc. Rev.*, 2009, **38**, 976.
3 F. Wang, R. Deng, J. Wang, Q. Wang, Y. Han, H. Zhu, X. Chen and X. Liu, *Nat. Mater.*, 2011, **10**, 968.
4 N. Souri, P. Tian, C. Platas-Iglesias, K.-L. Wong, A. Nonat and L. J. Charbonnière, *J. Am. Chem. Soc.*, 2017, **139**, 1456.
5 A. Nonat, S. Bahamyirou, A. Lecointre, F. Przybilla, Y. Mély, C. Platas-Iglesias, F. Camerel, O. Jeannin and L. J. Charbonnière, *J. Am. Chem. Soc.*, 2019, **141**, 1568.
6 A. M. Nonat and L. J. Charbonnière, *Coord. Chem. Rev.*, 2020, **409**, 213192.
7 L. J. Charbonnière, *Dalton Trans.*, 2018, **47**, 8566.
8 B. Golesorkhi, S. Naseri, L. Guenee, I. Taarit, F. Alves, H. Nozary and C. Piguet, *J. Am. Chem. Soc.*, 2021, **143**, 15326.
9 Y. Suffren, B. Golesorkhi, D. Zare, L. Guénée, H. Nozary, S. V. Eliseeva, S. Petoud, A. Hauser and C. Piguet, *Inorg. Chem.*, 2016, **55**, 9964.
10 B. Golesorkhi, H. Nozary, A. Fürstenberg and C. Piguet, *Mater. Horiz.*, 2020, **7**, 1279.
11 B. Golesorkhi, A. Fürstenberg, H. Nozary and C. Piguet, *Chem. Sci.*, 2019, **10**, 6876.
12 M. Kaiser, C. Würth, M. Kraft, I. Hyppänen, T. Soukka and U. Resch-Genger, *Nanoscale*, 2017, **9**, 10051.
13 C. Homann, L. Krukewitt, F. Frenzel, B. Grauel, C. Würth, U. Resch-Genger and M. Haase, *Angew. Chem., Int. Ed.*, 2018, **57**, 8765.
14 C. Würth, S. Fischer, B. Grauel, A. P. Alivisatos and U. Resch-Genger, *J. Am. Chem. Soc.*, 2018, **140**, 4922.
15 D. A. Gálico, C. M. S. Calado and M. Murugesu, *Chem. Sci.*, 2023, **14**, 5827.
16 K. Sheng, W.-D. Si, R. Wang, W.-Z. Wang, J. Dou, Z.-Y. Gao, L.-K. Wang, C.-H. Tung and D. Sun, *Chem. Mater.*, 2022, **34**, 4186.
17 D. A. Gálico and M. Murugesu, *ACS Appl. Mater. Interfaces*, 2021, **13**, 47052.
18 D. A. Gálico, A. A. Kitos, J. S. Ovens, F. A. Sigoli and M. Murugesu, *Angew. Chem., Int. Ed.*, 2021, **60**, 6130.
19 D. A. Gálico, R. Ramdani and M. Murugesu, *Nanoscale*, 2022, **14**, 9675.

20 D. A. Gálico and M. Murugesu, *Angew. Chem., Int. Ed.*, 2022, **61**, e202204839.
21 D. A. Gálico, J. S. Ovens, F. A. Sigoli and M. Murugesu, *ACS Nano*, 2021, **15**, 5580.
22 R. C. Knighton, L. K. Soro, A. Lecointre, G. Pilet, A. Fateeva, L. Pontille, L. Francés-Soriano, N. Hildebrandt and L. J. Charbonniere, *Chem. Commun.*, 2021, **57**, 53.
23 R. C. Knighton, L. K. Soro, L. Francés-Soriano, A. Rodríguez-Rodríguez, G. Pilet, M. Lenertz, C. Platas-Iglesias, N. Hildebrandt and L. J. Charbonniere, *Angew. Chem., Int. Ed.*, 2022, **61**, e202113114.
24 S. P. K. Panguluri, E. Jourdain, P. Chakraborty, S. Klyatskaya, M. M. Kappes, A. M. Nonat, L. J. Charbonnière and M. Ruben, *J. Am. Chem. Soc.*, 2024, **146**, 13083.
25 C. D. S. Brites, S. Balabhadra and L. D. Carlos, *Adv. Opt. Mater.*, 2019, **7**, 1801239.
26 K. Elzbieciak-Piecka, J. Drabik, D. Jaque and L. Marciniak, *Phys. Chem. Chem. Phys.*, 2020, **22**, 25949.
27 C. M. S. Calado, D. A. Gálico and M. Murugesu, *Chem. Commun.*, 2023, **59**, 13715.
28 M. Pollnau, D. R. Gamelin, S. R. Luthi and H. U. Güdel, *Phys. Rev. B: Condens. Matter Mater. Phys.*, 2000, **61**, 3337.
29 W. M. Yen, S. Shionoya and H. Yamamoto, *Phosphor handbook*, CRC Press, 2nd edn, 2007, pp. 844–885.
30 R. Sen, S. Paul, A. Sarkar, A. M. P. Botas, A. N. Carneiro Neto, P. Brandão, A. M. L. Lopes, R. A. S. Ferreira, J. P. Araújo and Z. Lin, *CrystEngComm*, 2021, **23**, 4143.
31 J. Zhou, B. Rosal, D. Jaque, S. Uchiyama, D. Jin, B. del Rosal, D. Jaque, S. Uchiyama and D. Jin, *Nat. Methods*, 2020, **17**, 967.
32 C. D. S. Brites, R. Marin, M. Suta, A. N. C. Neto, E. Ximendes, D. Jaque and L. D. Carlos, *Adv. Mater.*, 2023, **35**, 2302749.
33 N. F. Mott, *Proc. R. Soc. A*, 1938, **167**, 384.
34 F. Seitz, *Trans. Faraday Soc.*, 1939, **167**, 74.
35 D. A. Gálico, E. R. Souza, I. O. Mazali and F. A. Sigoli, *J. Lumin.*, 2019, **210**, 397.
36 G. M. Salley, R. Valiente and H. U. Güdel, *J. Phys.: Condens. Matter.*, 2002, **14**, 5461.